Appl. Phys. A (2015) 120:693–698
DOI 10.1007/s00339-015-9241-x

Applied Physics A
Materials Science & Processing

Supercapacitors based on highly dispersed polypyrrole-reduced graphene oxide composite with a folded surface

Anqi Wang[1] · Xi Zhou[1] · Tao Qian[1] · Chenfei Yu[1] · Shishan Wu[1] · Jian Shen[1,2]

Received: 13 November 2014 / Accepted: 18 May 2015 / Published online: 26 May 2015

Abstract Highly dispersed polypyrrole particles were decorated on reduced graphene oxide sheets using a facile in situ synthesis route. The prepared composite, which obtained a folded surface, shows remarkable performance as the electrode material of supercapacitors. The specific capacitance reaches 564.1 F g^{-1} at a current density of 1 A g^{-1} and maintains 86.4 % after 1000 charging–discharging cycles at a current density of 20 A g^{-1}, which indicates a good cycling stability. Furthermore, the prepared supercapacitor demonstrates an ultrahigh energy density of 50.13 Wh kg^{-1} at power density of 0.40 kW kg^{-1}, and remains of 45.33 Wh kg^{-1} even at high power density of 8.00 kW kg^{-1}, which demonstrate that the hybrid supercapacitor can be a promising energy storage system for fast and efficient energy storage in the future.

1 Introduction

The fast growth of portable electronic devices and electric vehicles stimulates the increasing demand for high-energy storage resources in recent years [1–3]. Supercapacitors, also known as ultracapacitors or electrochemical capacitors, have attracted considerable attention due to their higher power density than batteries and higher energy density than traditional dielectric capacitors [4–8]. A supercapacitor stores energy through charge accumulation at the electrode–electrolyte interface. Such a charge storage mechanism requires the electrode material to have a sufficiently high surface area and a good electrical conductivity.

Graphene consisting of a two-dimensional sheet of covalently bonded carbon atoms has high electronic conductivity, low mass density, high specific surface area [9–11] and finds a multitude of applications in devices [12–14]. Since the first successful fabrication of a graphene-based supercapacitor in 2006, nanocomposite electrode materials based on graphene [15–20] and other active materials have attracted great interest. Reduced graphene oxide (RGO), one kind of chemically derived graphene, has shown similar characteristics to graphene in many aspects [21]. However, the substantial loss in oxygen-containing groups of graphene oxide (GO) after the chemical reduction largely lowers the electrostatic repulsions between the sheets, resulting in an agglomeration, which not only decreases the surface area, but also precludes the access of electrolyte ions to the surface of the RGO sheets [22]. To minimize the restacking of RGO sheets, recent developments have focused on constructing secondary structures on RGO sheets in order to enlarge the surface area for charge storage [23, 24].

Conducting polymers have been extensively studied in supercapacitors owing to their fast doping/undoping process. Polypyrrole (PPy), one of the most important conducting polymers, has been treated as a potential material for supercapacitors due to its good conductivity, low cost, stability, high redox pseudocapacitive charge storage, and

Electronic supplementary material The online version of this article (doi:10.1007/s00339-015-9241-x) contains supplementary material, which is available to authorized users.

✉ Shishan Wu
shishanwu@nju.edu.cn

[1] School of Chemistry and Chemical Engineering, Nanjing University, Nanjing 210093, China

[2] College of Chemistry and Materials Science, Nanjing Normal University, Nanjing 210097, China

accessibility by facial synthesis [25–27]. The existence of a positive surface charge on the PPy provides an interface for the interaction of modified materials. In the present work, highly dispersed PPy–RGO composite (HPG) has been fabricated through in situ chemical oxidative polymerization on the surface of GO sheets by the initiation of $FeCl_2$/H_2O_2 and then reduced by hydrazine. The electrostatic repulsive interaction between decorative highly dispersed PPy (HP) prevents the aggregation of RGO sheets, which lead to a high dispersibility of HPG composite. Meanwhile, during the composite process, the RGO sheets dramatically turn into folded structure, which probably change its form/phase and functionality, and thus induce new and distinct properties [28]. As a result, the unique high dispersibility and folded structure of HPG provide a promising potential of this material for practical application in supercapacitors.

2 Experimental section

2.1 Materials

Pyrrole (AR) and hydrogen peroxide (H_2O_2, 30 %, AR) were purchased from Sinopharm Chemical Reagent Co. (China). $FeCl_2$ and hydrazine hydrate (80 %, AR) were purchased from Shanghai Chemical Reagent Co. (China). Deionized water was applied for all polymerization and reaction processes.

2.2 Synthesis of HPG hybrids

GO was synthesized using a modified Hummer's method [29] and dispersed in water with a concentration of 1.0 mg/1.0 g H_2O by ultrasonication. Nanocomposite was synthesized using in situ polymerization in the presence of GO suspension and pyrrole with different ingredient mass ratios from 2:1 to 1:4 for pyrrole and GO. The hybrid material synthesized from different ratios is denoted as HPG21, HPG11, HPG12, and HPG14, which indicate that the mass ratio of HP and RGO is 2:1, 1:1, 1:2, and 1:4, respectively. Here, we take the HPG12 composite as an example, the procedure is as follows: In situ polymerization was initiated with the addition of 0.25 mL H_2O_2 to the GO/pyrrole/$FeCl_2$/H_2O (0.1 g/0.05 mL/0.005 g/100 mL) mixture and lasted for 6 h. HPG12 composite was then obtained by the reduction of hydrazine and dispersed in water at a concentration of 0.1 wt%.

2.3 Characterization

Scanning electron microscopy (SEM) imaging was performed on a JEOL-JSM-7600F SEM. Zeta potential was recorded on a Malvern Nano-Z Instrument. X-ray photoelectron spectroscopy (XPS) measurements are taken on a PHI 5000 VersaProbe. All electrochemical characteristics were evaluated by cyclic voltammetry (CV) and galvanostatic charge–discharge measurements on a CHI660d (Shanghai CH Instrument Company, China). The electrochemical cell used was a conventional three-electrode cell with a bare or modified glassy carbon electrode (GCE; diameter = 3 mm) as the working electrode, a saturated calomel electrode (SCE) as the reference electrode and a platinum wire as the counterelectrode in 1 M KCl solution.

3 Results and discussion

Figure 1 shows the photograph of HP, RGO, and HPG composite dispersion. All of the dispersions were placed for 24 h after ultrasonication to reveal the dispersibility directly perceived through naked eye. It can be seen clearly that the HP dispersion is stably dispersed in aqueous solvent. However, we failed to prepare stable RGO sheets due to the loss in substantial oxygen-containing groups. Amazingly, it is found that the HPG composite dispersion exhibits no sedimentation or aggregation and they remained stable and homogeneous for more than 3 months. These phenomena illustrate that the decorative HP prevents the aggregation of RGO sheets by electrostatic repulsive interaction between them, leading to a high dispersibility of HPG composites. The data of zeta potentials are presented in Table 1, and the result is according to that of above, which further confirms the improvement of electrostatic repulsive interaction between the prepared sheets.

To investigate the morphology of the fabricated HPG hybrids with different weight ratio of HP, SEM images

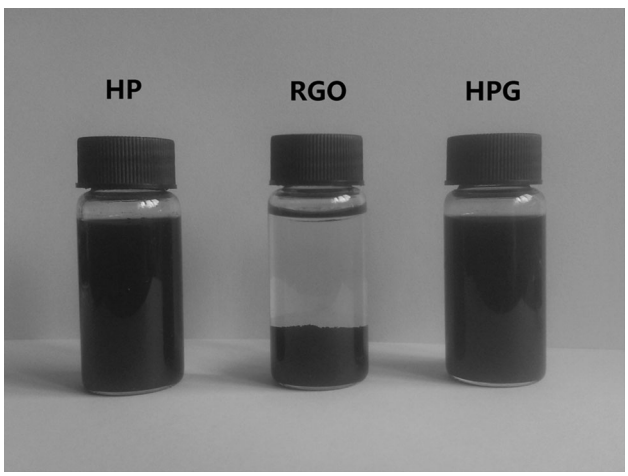

Fig. 1 Photographs of HP, RGO sheets, and HPG composite dispersed in water (2 mg mL^{-1}) after 1-h ultrasonication and stand for 24 h, pH 7.0

Table 1 Zeta potential data of RGO and HPG composites

	RGO	HPG21	HPG11	HPG12	HPG14
Zeta potential (mV), pH 7.0	−3.5	−39.5	−38.8	−37.9	−37.7

were taken and results are shown in Fig. 2. It is obvious that the RGO sheets are separated into smaller-scale ones with the excess decoration of HP particles (Fig. 2a, b), as a result of the electrostatic repulsive interaction between plentiful nanoparticles. However, the surfaces of the hybrid films are still smooth and little crumple can be observed. By contrast, Fig. 2c, d shows an integrated RGO sheet, especially revealing the abundant crumple and wrinkle structures on the surface of HPG12 film, which could extremely promote the surface area of the hybrids.

XPS is a powerful technique to discern the surface chemical species of materials. Therefore, the synthesized HPG hybrid material has been subjected to XPS analysis (Fig. S1). From careful inspection of wide region spectroscopy (Fig. S1A) of GO and HPG composite from XPS study, it is observed that the C/O ratio is 0.57 for GO sheets and 1.50 for HPG, which is mainly due to the addition of HP and the remove of most of oxygen functionality after reduction. In addition, the peak of N 1 s in the HPG is obviously observed, corroborating the presence of HP in the concerned composites. The high-resolution XPS spectra for the C 1 s of GO (Fig. S1B) indicates the presence of four types of carbon bonds: C–C (284.5 eV), C–O (286.6 eV), C=O (288.4 eV), and O=C–O (291.0 eV). After reduction, the peak associated with C–C (284.5 eV) becomes predominant, while the peaks related to the oxidized carbon species are greatly weakened (Fig. S1C). From Fig. S1D, it can be seen that the only peak at 399.5 eV corresponds to high-resolution XPS spectrum of N atoms within the pentagonal ring of the HP for HPG hybrids [30, 31]. These results reflect that the HP is decorated on RGO sheets and further confirmed the surface component of prepared hybrids.

The electrochemical performance of the samples as the electrode material for supercapacitors was tested by CV and galvanostatic charge–discharge technique in three-electrode system. Figure 3a shows the CV curves of HPG12 with different scan rates in 1 M KCl aqueous

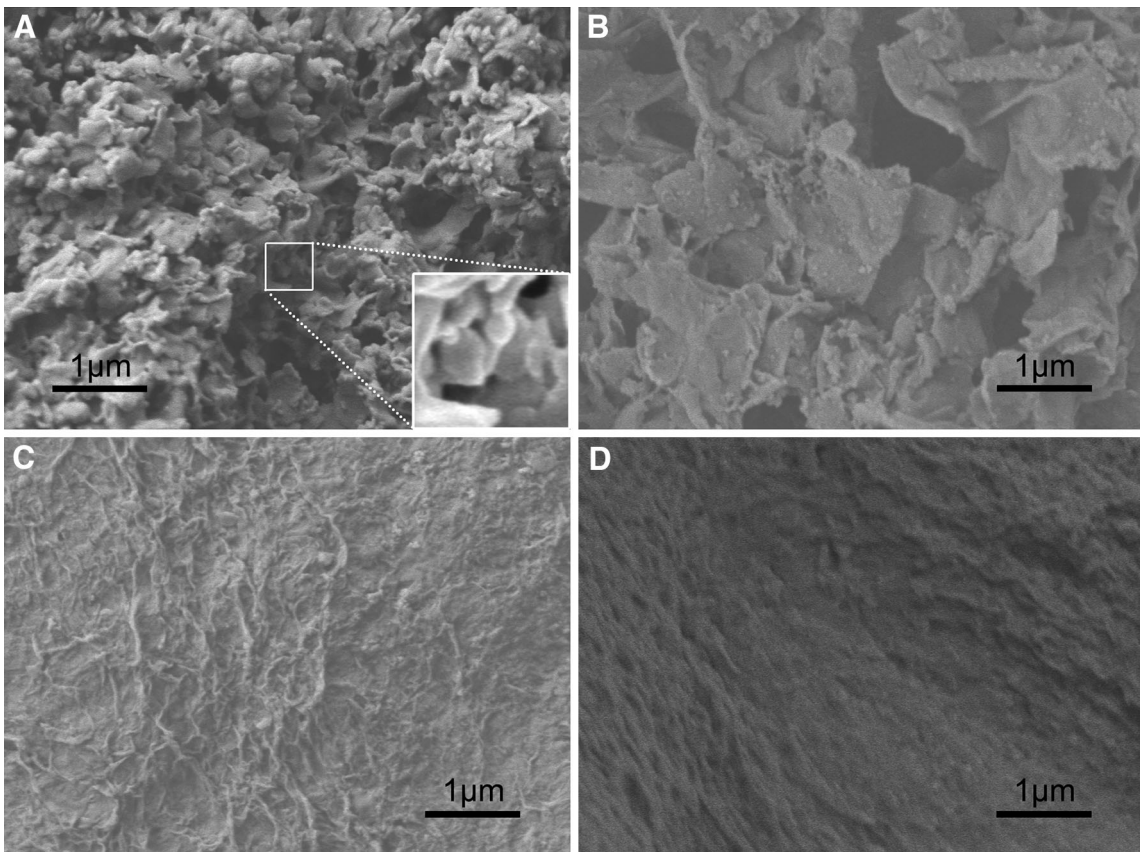

Fig. 2 SEM images of HPG composite films with HP/RGO weight ratio of **a** 2:1, **b** 1:1, **c** 1:2, and **d** 1:4, respectively

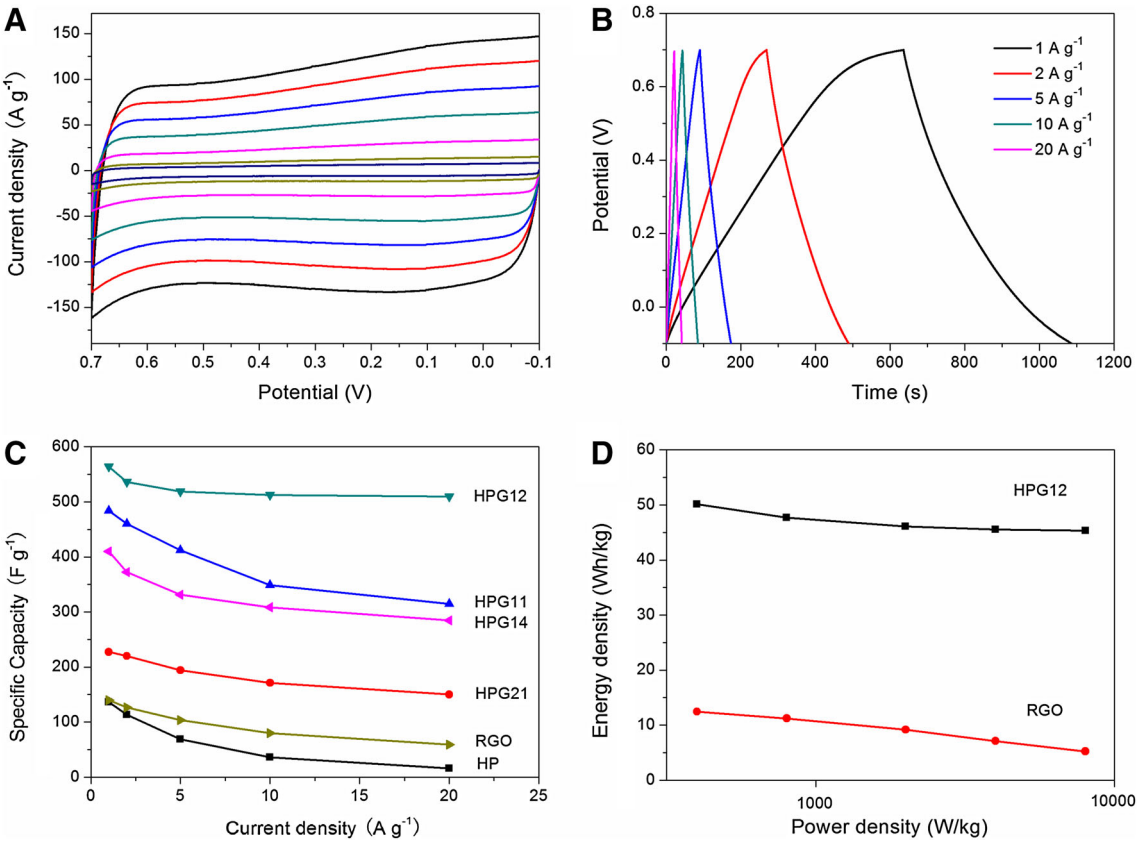

Fig. 3 **a** CVs of HPG12 electrode in 1.0 M KCl solution between −0.1 and 0.7 V at different scan rates. **b** Galvanostatic charge–discharge curves of HPG12 supercapacitor with different current densities. **c** The specific capacitances of HP-, RGO-, and HPG-modified electrodes at different current densities. **d** Ragone plots of HPG12 and RGO sheets

solution. All the results exhibit rectangular and symmetric CV curves, which prove the ideal capacitive nature with fast charge–discharge process. Galvanostatic cycling of the modified electrode was performed at different current densities. As seen in Fig. 3b, the discharge curves are approximately linear in the total range of potential, showing nearly perfect capacitive behavior. The capacitance of HPG12 was evaluated from the discharge curves, which was 564.1 F g^{-1} at a discharge current density of 1 A g^{-1}, and the capacitance was 510.4 F g^{-1} when the discharge current density increased to 20 A g^{-1}, which is a fairly high current density, leaving only a 9.5 % loss with a 2000 % increase in the discharge current density (Fig. 3c). Therefore, these results show that the addition of HP plays a significant role in improving the electrochemical performance of the RGO sheets, which results in 57.9 % loss with a same increase in the discharge current density. It is worth noting that the specific capacitance of the HPG12 is higher than that of the HPG composites with other weight ratios (Fig. S2), which is influenced by the multifactor, mainly the surface area and the conductivity of material itself. With the decreasing amount of PPy, crumple on HPG reduces, resulting in the decrease in surface area and that of capacitance. However, at the same time, the conductivity of HPG itself suffers due to the low conductivity of PPy comparing to RGO sheets. Given all that, the HPG12 has the most appropriate ratio of PPy and RGO, which leads to the highest capacitance among these products. And the superior capacitance of HPG under high current density indicates its potential appliance in this supercapacitor which needs rapid charge–discharge process.

Ragone plot is a chart used for performance comparison of various energy-storing devices [32]. Ragone plots for the devices fabricated with pristine RGO and HPG12 are shown in Fig. 3d, which are calculated using galvanostatic charge–discharge data acquired at different current densities. The RGO electrode delivers energy density as low as 12.44 Wh kg^{-1} even at a power density of 0.40 kW kg^{-1} because of its low specific capacitance. In contrast, the HPG12 composite supercapacitor shows a significant enhancement of energy density, which delivered 50.13 Wh kg^{-1} at the power density of 0.40 kW kg^{-1}. More importantly, the energy density of prepared capacitor is very stable with the increase in the power density, which reaches up to 45.33 Wh kg^{-1} even at a power density as high as 8.00 kW kg^{-1}. Compared to several recent studies

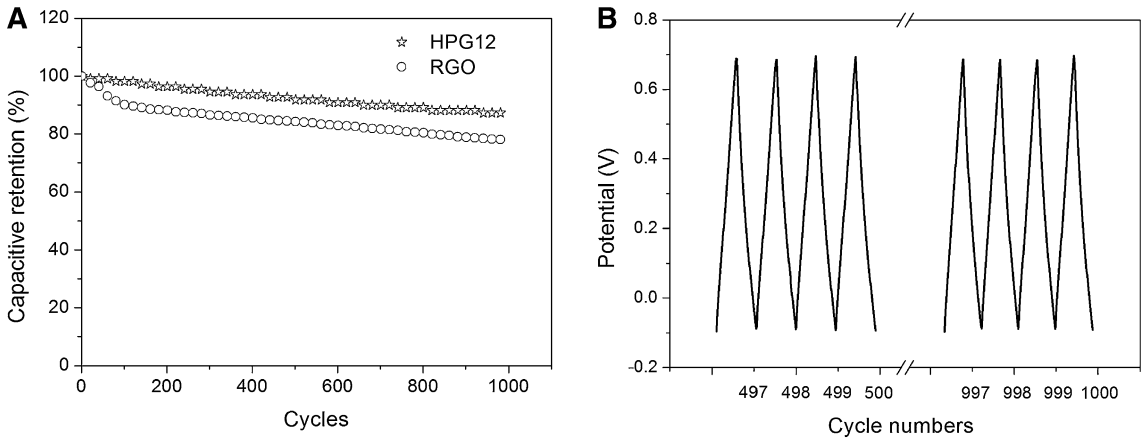

Fig. 4 **a** Cycle stability of HPG12 and RGO sheets during the long-term charge–discharge process. **b** Charge–discharge profile of HPG12-modified electrode for the middle four cycles and last four cycles at a current density of 20 A g^{-1}

[33, 34], our HPG composite supercapacitor has a higher power density.

Another important requirement for supercapacitor applications is cycling capability or cycling life. The cycling life tests over 1000 cycles for the RGO and HPG12 electrodes at a current density of 20 A g^{-1} were carried out using constant current galvanostatic charge–discharge cycling techniques in the potential windows ranging from −0.1 to 0.7 V. Figure 4a shows the specific capacitance retention as a function of cycle number. The specific capacitance of pristine RGO remains only 77.6 % after 1000 charge–discharge cycles. By contrast, the HPG12-modified electrode shows a slight decrease and its capacitance still remains about 86.4 %, which demonstrates a higher cycling stability. The good long-term electrochemical stability of HPG12 hybrids is further evident from the stable charge–discharge curves for the middle four cycles and last four cycles (Fig. 4b). The curve shape of the latter is similar to that of the former (497–500 cycles), which remains essentially symmetric triangle shape.

4 Conclusions

In conclusion, HPG composite has been successfully prepared via an in situ chemical oxidative polymerization process, which endows the RGO sheets unique folded surface structure. Being employed as a supercapacitor, such composite exhibits excellent specific capacity (564.1 F g^{-1} at a current density of 1 A g^{-1}, remains 510.4 F g^{-1} at a current density of 20 A g^{-1}) and cycling stability (the capacitive retention was 86.4 % after 1000 cycles). The exceptional performance can be attributed to the high dispersibility and existence of sufficient crumples, which can enhance the surface area. This unique composite is promising to act as a new candidate for an electrode material for high-performance supercapacitors.

Acknowledgments This work was supported by the National Natural Science Foundation of China (Nos. 51272100 and 51273073) and the Foundation of Jiangsu Collaborative Innovation Center of Biomedical Functional Materials.

References

1. F.B. Sillars, S.I. Fletcher, M. Mirzaeian, P.J. Hall, Effect of activated carbon xerogel pore size on the capacitance performance of ionic liquid electrolytes. Energy Environ. Sci. **4**, 695–706 (2011)
2. L.L. Zhang, X.S. Zhao, Carbon-based materials as supercapacitor electrodes. Chem. Soc. Rev. **38**, 2520–2531 (2009)
3. J.R. Miller, P. Simon, Electrochemical capacitors for energy management. Science **321**, 651–652 (2008)
4. H. Wang, H.S. Casalongue, Y. Liang, H. Dai, $Ni(OH)_2$ nanoplates grown on graphene as advanced electrochemical pseudocapacitor materials. J. Am. Chem. Soc. **32**, 7472–7477 (2010)
5. Z. Chen, Y. Qin, D. Weng, Q. Xiao, Y. Peng, X. Wang, H. Li, F. Wei, Y. Lu, Design and synthesis of hierarchical nanowire composites for electrochemical energy storage. Adv. Funct. Mater. **19**, 3420–3426 (2009)
6. Z. Fan, J. Yan, T. Wei, L. Zhi, G. Ning, T. Li, F. Wei, Asymmetric supercapacitors based on graphene/MnO_2 and activated carbon nanofiber electrodes with high power and energy density. Adv. Funct. Mater. **21**, 2366–2375 (2011)
7. L.H. Bao, J.F. Zang, X.D. Li, Flexible Zn_2SnO_4/MnO_2 core/shell nanocable carbon microfiber hybrid composites for high-performance supercapacitor electrodes. Nano Lett. **11**, 1215–1220 (2011)
8. Z. Chen, V. Augustyn, J. Wen, Y.W. Zhang, M.Q. Shen, B. Dunn, Y.F. Lu, High-performance supercapacitors based on intertwined CNT/V_2O_5 nanowire nanocomposites. Adv. Mater. **23**, 791–795 (2011)
9. O.C. Compton, S. Kim, C. Pierre, J.M. Torkelson, S.T. Nguyen, Crumpled graphene nanosheets as highly effective barrier property enhancers. Adv. Mater. **22**, 4759–4763 (2011)

10. D.R. Dreyer, S. Park, C.W. Bielawski, R.S. Ruoff, The chemistry of graphene oxide. Chem. Soc. Rev. **39**, 228–240 (2010)
11. L. Yan, Y.B. Zheng, F. Zhao, S. Li, X. Gao, B. Xu, Chemistry and physics of a single atomic layer: strategies and challenges for functionalization of graphene and graphene-based materials. Chem. Soc. Rev. **41**, 97–114 (2012)
12. X. Li, H. Wang, J.T. Robinson, T. Sanchez, G. Diankov, H. Dai, Simultaneous nitrogen doping and reduction of graphene oxide. J. Am. Chem. Soc. **131**, 15939–15944 (2009)
13. L.T. Qu, Y. Liu, J.B. Baek, L.M. Dai, Nitrogen-doped graphene as efficient metal-free electrocatalyst for oxygen reduction in fuel cells. ACS Nano **4**, 1321–1326 (2010)
14. Z.S. Wu, W. Ren, L. Gao, J. Zhao, Z. Chen, B. Liu, Synthesis of graphene sheets with high electrical conductivity and good thermal stability by hydrogen arc discharge exfoliation. ACS Nano **3**, 411–417 (2009)
15. X. Zhou, X. Huang, X. Qi, S. Wu, C. Xue, F.Y.C. Boey, Q. Yan, P. Chen, H. Zhang, In situ synthesis of metal nanoparticles on single-layer graphene oxide and reduced graphene oxide surfaces. J. Phys. Chem. C **113**, 10842–10846 (2009)
16. H. Gómez, M.K. Ram, F. Alvi, P. Villalba, E. Stefanakos, A. Kumar, Graphene-conducting polymer nanocomposite as novel electrode for supercapacitors. J. Power Sources **196**, 4102–4108 (2011)
17. Z. Yin, S. Wu, X. Zhou, X. Huang, Q. Zhang, F. Boey, H. Zhang, Electrochemical deposition of ZnO nanorods on transparent reduced graphene oxide electrodes for hybrid solar cells. Small **6**, 307–312 (2010)
18. K.S. Kim, Y. Zhao, H. Jang, S.Y. Lee, J.M. Kim, K.S. Kim, J.H. Ahn, P. Kim, J.Y. Choi, B.H. Hong, Large-scale pattern growth of graphene films for stretchable transparent electrodes. Nature **457**, 706–710 (2009)
19. C. Berger, Z.M. Song, X.B. Li, X.S. Wu, B. Brown, C. Naud, D. Mayou, T.B. Li, J. Hass, A.N. Marchenkov, E.H. Conrad, P.N. First, W.A. de Heer, Electronic confinement and coherence in patterned epitaxial graphene. Science **312**, 1191–1196 (2006)
20. C. Gomez-Navarro, R.T. Weitz, A.M. Bittner, M. Scolari, A. Mews, M. Burghard, K. Kern, Electronic transport properties of individual chemically reduced graphene oxide sheets. Nano Lett. **7**, 3499–3503 (2007)
21. S.F. Pei, H.M. Cheng, Effects of reduction process and carbon nanotube content on the supercapacitive performance of flexible graphene oxide papers. Carbon **50**, 4239–4251 (2012)
22. D. Li, M.B. Müller, S. Gilje, R.B. Kaner, G.G. Wallace, Processable aqueous dispersions of graphene nanosheets. Nat. Nanotechnol. **3**, 101–105 (2008)
23. C. Liu, Z. Yu, D. Neff, A. Zhamu, B.Z. Jang, Graphene-based supercapacitor with an ultrahigh energy density. Nano Lett. **10**, 4863–4868 (2010)
24. Y. Zhu, S. Murali, M.D. Stoller, K.J. Ganesh, W. Cai, P.J. Ferreira, A. Pirkle, R.M. Wallace, K.A. Cychosz, M. Thommes, D. Su, E.A. Stach, R.S. Ruoff, Carbon-based supercapacitors produced by activation of grapheme. Science **332**, 1537–1541 (2011)
25. J.H. Kim, A.K. Sharma, Y.S. Lee, Synthesis of polypyrrole and carbon nano-fiber composite for the electrode of electrochemical capacitors. Mater. Lett. **60**, 1697–1701 (2006)
26. R.K. Sharma, A.C. Rastogi, S.B. Desu, Manganese oxide embedded polypyrrole nanocomposites for electrochemical supercapacitor. Electrochim. Acta **53**, 7690–7695 (2008)
27. A.R. Liu, C. Li, H. Bai, G.Q. Shi, Electrochemical deposition of polypyrrole/sulfonated graphene composite films. J. Phys. Chem. C **114**, 22783–22789 (2010)
28. A. Ambrosi, A. Bonanni, M. Pumera, Electrochemistry of folded graphene edges. Nanoscale **3**, 2256–2260 (2011)
29. W.S. Hummers, R.E. Offeman, Preparation of graphitic oxide. J. Am. Chem. Soc. **80**, 1339 (1958)
30. S. Shrestha, W.E. Mustain, Properties of nitrogen-functionalized ordered mesoporous carbon prepared using polypyrrole precursor. J. Electrochem. Soc. **157**, B1665–B1672 (2010)
31. F. Kapteijn, J.A. Moulijn, S. Matzner, H.P. Boehm, The development of nitrogen functionality in model chars during gasification in CO_2 and O_2. Carbon **37**, 1143–1150 (1999)
32. Ramaprabhu S. Jaidev, Poly(p-phenylenediamine)/graphene nanocomposites for supercapacitor applications. J. Mater. Chem. **22**, 18775–18783 (2012)
33. Y.H. Wu, C.X. Guo, N. Li, L.L. Ji, Y.F. Tu, X.M. Yang, Three-dimensional interconnected nanocarbon hybrid prepared by one-pot synthesis method with polypyrrole-based nanotube and graphene and the application in high-performance capacitance. Electrochim. Acta **146**, 386–394 (2014)
34. W.H. Khoh, J.D. Hong, Solid-state asymmetric supercapacitor based on manganese dioxide/reduced-graphene oxide and polypyrrole/reduced-graphene oxide in a gel electrode. Colloid Surf. A **456**, 26–34 (2014)